ORIGINAL RESEARCH

MALAT1 exacerbates immune dysregulation in gestational diabetes by modulating the miR-576-5p/HNRNPU axis: Implications for inflammatory pathogenesis

Hui Ding, Anna Zhao, Xia Chen, Yanli Niu, Yuanyuan Wang, Xiao Chen, Hong Yang*

Department of Obstetrics, Xuyi County People's Hospital, Xuyu, Huai'an, Jiangsu 211700, China.

*** Corresponding Author:Hong Yang**; E-mail: yanghong_edu@outlook.com

Abstract

Background

Gestational diabetes mellitus (GDM) is characterized by systemic immune dysregulation and chronic inflammation that contribute to insulin resistance and β-cell dysfunction. The long non-coding RNA metastasis-associated lung adenocarcinoma transcript 1 (MALAT1) has been implicated in several inflammatory disorders; however, its role in GDM-related immune and metabolic disturbances remains unclear.

Methods

A mouse model of GDM and insulin-resistant trophoblast cells were used to evaluate MALAT1 expression and its effects on inflammatory cytokines and β-cell apoptosis. Gene expression was analyzed by qRT-PCR and Western blotting, while histological and biochemical assays assessed pancreatic morphology, serum glucose, and inflammatory cytokine levels. Functional and rescue experiments were performed to explore the molecular interaction between MALAT1, miR-576-5p, and HNRNPU.

Results

MALAT1 expression was markedly elevated in GDM mice and insulin-resistant trophoblasts, correlating with increased levels of TNF-α, IL-1β, and IL-6, as well as enhanced β-cell apoptosis. Silencing MALAT1 alleviated hyperglycemia, preserved pancreatic islet structure, and reduced inflammatory mediator secretion. Mechanistically, MALAT1 acted as a competing endogenous RNA by sponging miR-576-5p to upregulate HNRNPU, thereby promoting NF-κB activation. HNRNPU overexpression reversed the anti-inflammatory and anti-apoptotic effects of MALAT1 knockdown.

Conclusion

MALAT1 promotes immune-metabolic dysfunction in GDM through the miR-576-5p/HNRNPU/NF-κB axis. Targeting this pathway may offer a novel therapeutic strategy for reducing inflammation-associated complications in GDM.

Keywords: Gestational diabetes mellitus, MALAT1, HNRNPU, miR-576-5p, immune dysregulation, pro-inflammatory cytokines

Introduction

Gestational diabetes mellitus (GDM) is widely acknowledged to be a common complication encountered in the time of pregnancy, and is marked by glucose intolerance, a condition that either manifests for the first time or is initially detected during the gestational period[1]. This condition has a significant global impact, affecting roughly 15% of pregnant women worldwide. GDM not merely a temporary concern during pregnancy; rather, it carries substantial risks for both the mother and the developing fetus. Moreover, women who suffer from GDM have an elevated risk of developing type 2 diabetes mellitus (T2DM) along with cardiovascular diseases in the postpartum period[2]. Currently, the management of GDM primarily revolves around dietary adjustments and pharmacological interventions, including the use of metformin and insulin[3]. Research indicates that GDM patients often exhibit varying degrees of insulin resistance (IR) or insufficient insulin secretion[4]. IR denotes a diminished responsiveness of target organs to insulin[5]. On a molecular level, IR manifests as a reduced ability of insulin, whether naturally circulating or externally administered, to lower blood glucose levels[6]. While some degree of IR is a normal physiological adaptation during pregnancy, facilitating the transfer of glucose from the mother to the fetus and supporting normal fetal growth and development, severe IR can lead to maternal hyperglycemia[7]. Consequently, delving into the pathogenesis of IR assumes paramount importance in the quest for effective GDM treatments.

Long non-coding RNAs (lncRNAs) constitute a unique subset of functional RNA molecules. They are distinguished by their extended length, typically exceeding 200 nucleotides, and notably lack the ability to encode proteins[8]. These RNA entities exert regulatory influence over protein-coding genes through a variety of sophisticated mechanisms[9]. For instance, they can form intricate complexes with their target genes, thereby modulating gene activity[10]. Additionally, lncRNAs are capable of interacting with microRNAs (miRNAs), either promoting their degradation or impeding their translation and post-transcriptional modification processes[11]. LncRNAs have a pervasive role in both the physiological and

pathological aspects that occur within the body. They are crucial for sustaining cellular homeostasis, ensuring that cells function optimally under normal conditions. Additionally, lncRNAs are instrumental in the body's response to disease states, helping to regulate and potentially mitigate the effects of various pathologies[12]. Numerous studies have manifested that aberrant lncRNA expression profiles are closely related to the pathogenesis of complex diseases, including cancer, cardiovascular disease, neurological disease and diabetes[13]. The expanding corpus of knowledge on lncRNAs not only enhances our comprehension of the mechanisms underlying diseases but also paves the way for the creation of tailored therapeutic approaches and the identification of diagnostic biomarkers[14].

LncRNA metastasis-associated lung adenocarcinoma transcript 1 (MALAT1) belongs to one of the most extensively investigated and evolutionarily conserved lncRNAs and is located on the short arm of human chromosome 11q13.1[15]. A substantial body of research has established its significant involvement in a myriad of pathological processes, spanning diabetes and an array of malignant neoplasms[16,17]. Notably, it has been documented that MALAT1 expression is higher among GDM patients than pregnant women without GDM[18]. Besides, Abdulle and his colleague suggested that MALAT1 expression showed upregulation in different diabetic-related diseases, GDM included[19]. However, the specific function and related mechanism of MALAT1 in regulating IR in GDM still warrant further clarification.

Consequently, the current research aimed to explore the role and molecular intricacies of MALAT1 in governing IR during GDM. Based on our findings, it is plausible to hypothesize that fluctuations in MALAT1 expression levels could potentially offer valuable insights into developing novel therapeutic methods for GDM.

Material and methods

Ethics statement

The care and handling of mice throughout this study adhered strictly to the guidelines and protocols sanctioned by the Institutional Animal Care and Use Committee of our hospital. Every possible measure was taken to ensure that the experimental mice experienced minimal unnecessary distress or suffering.

Construction of GDM mouse model

Cyagen (Suzhou) Biotechnology Co., Ltd., Suzhou, China provided seven-week-old female (weighing 16-17 g) as well as male C57BL/6J mice (weighing 17-18 g). The mice were kept in an environment with precisely regulated conditions. They were housed at a temperature that stayed within the range of 20-25%, while the relative humidity was consistently maintained between 45%-55%. Additionally, they were exposed to a 12-hour light/dark cycle to mimic natural day-night patterns. After a one-week acclimation period, mice were randomly assigned to experimental or control groups.

The control group consisted exclusively of age-matched pregnant female mice housed under identical conditions as the experimental group. Male mice were not included in the control group. To confirm pregnancy, female mice were cohabited with males at a 2:1 ratio overnight. Pregnancy was verified via vaginal smear for sperm detection, with the day of confirmation designated as gestation day 0 (GD0).

On GD6, the pregnant mice received an intraperitoneal injection of streptozocin (40 mg/kg, Sigma, USA), following a previously established protocol[20]. Blood samples were gathered from the tail vein of each mouse. The blood glucose levels were measured utilizing the glucose oxidase-peroxidase method. Mice exhibiting blood glucose levels ≥ 11.1 mmol/L within 48 hours of the injection, and maintaining this level for three consecutive days, were deemed to have successfully developed the experimental model.

Animal grouping

A total of 24 mice that had been successfully modeled were randomly and evenly separated into 4 groups, with every group comprising six mice. The groups were as follows: the control group; the GDM group, which consisted of GDM-induced mice; the GDM+sh-NC group, where GDM mice received an injection of sh-NC; and the GDM+sh-MALAT1 group, in which GDM mice were injected with sh-MALAT1. Both the sh-NC and sh-MALAT1 were prepared at a concentration of 20 μg and dissolved in 2.5 mL of normal saline prior to administration. The solutions were then injected into the tail veins of the respective mice. As a control, an additional six normal pregnant mice were included in the study and designated to be the normal group. Mice in both normal and GDM groups were administered an equal volume of normal saline via tail-vein injection. On the 18th day of gestation (GD18), the mice were anesthetized and euthanized. The pancreatic tissues were then carefully harvested and utilized for the relevant experimental detections.

Detection of glucose and insulin

The fasting blood glucose (FBG) levels were determined using the glucose oxidase-peroxidase method, with the assay kit sourced from Sigma, USA. To measure the fasting serum insulin (FINS) levels, enzyme-linked immunosorbent assay (ELISA) kits tailored for mouse insulin, produced by Beyotime, China, were utilized. Using the measured FBG and FINS values, the homeostatic model assessment-insulin resistance index (HOMA-IR) was computed following the formula (FBG × FINS)/22.5.

Hematoxylin-eosin (HE) staining

Following fixation of the pancreatic tissues using 4% paraformaldehyde overnight, the tissue was thoroughly rinsed with running water for 4 hours to remove any residual fixative. Subsequently, the tissues were dehydrated utilizing a train of ethanol solutions with increasing concentrations. This was followed by a 30-minute treatment with xylene to further prepare the tissue for embedding. The dehydrated tissue was then embedded in paraffin wax. Using a microtome, the paraffin-embedded tissue was cut into 5 μm-thick sections. These sections were subjected to deparaffinization by immersion in xylene for 15 minutes, followed by a train of ethanol washes. Next, the sections were then stained with hematoxylin (obtained from Solarbio, China) for 5 minutes to highlight the nuclei. After a brief rinse, the sections were counterstained with eosin (sourced from Sangon, China) for 3 minutes. Finally, the stained sections were dehydrated once more using a graded ethanol series and xylene. The sections were then mounted on glass slides and examined utilizing a microscope (Olympus, Tokyo, Japan).

TUNEL staining

Utilizing TUNEL kits (Beyotime, China), apoptosis in pancreatic tissues was assessed. The tissue samples underwent a series of preparatory steps: first, they were

dewaxed and hydrated, followed by a 30-minute incubation with proteinase K. Subsequently, the tissues were treated with TUNEL solution (Beyotime, China) for a duration of 1 hour. The proportion of TUNEL positive cells was observed utilizing a microscope (Olympus, Japan).

Cell culture

Wuhan Pricella Biotechnology Co., Ltd (Wuhan, China) supplied the human extravillous trophoblast cell line, HTR-8/SVneo. Cells were kept in RPMI-1640 (Gibco, USA) which contained 10% fetal bovine serum (Gibco, USA) at 37°C in 5% CO2. To stimulate IR, cells were treated with insulin (Solarbio, China) of 10-6 mol/l for 48 h as mentioned previously[21].

Cell transfection

GenePharma company (Shanghai, China) suppled the MALAT1 short hairpin RNA (sh-MALAT1) and shRNA negative control (sh-NC), miR-576-5p mimics and NC mimics, as well as the overexpression plasmids of HNRNPU and MALAT1 (pcDNA3.1-HNRNPU and pcDNA3.1-MALAT1) and empty vector (pcDNA3.1). Cell transfections were performed using lipofectamine 3000.

RT-qPCR

Utilizing TRIzol reagent, total RNA was extracted from pancreatic tissues and cells, strictly adhering to the instructions. The extracted RNA was then subjected to reverse transcription utilizing the PrimeScript RT Master Mix Kit (TAKARA, Japan). Subsequently, RT-qPCR was carried out. The reaction was performed with SYBR Green Master Mix on the Roche Real-time PCR system. To ensure accurate quantification of gene expression, GAPDH or U6 was employed to be an internal control gene. The relative expression levels were calculated utilizing the comparative Ct (2-ΔΔCT) methods.

Cell counting kit-8 (CCK-8)

Cells (1×103 cells per milliliter) were detached from the culture surface through trypsinization and subsequently planted into 96-well cell culture plates. To evaluate cell viability, at the 24, 48 and 72 h time points post-culture, 10 μL of CCK-8 reagent (sourced from DOJINDO Laboratories, Japan) was employed to add into each well for 3 hours of culture. The optical density at a wavelength of 450 nm was measured using a microplate reader.

Colony formation

Cells (5 × 102 cells per well) were carefully seeded into 6-well plates. The plates were then placed in an incubator and cultured for 14 days. Following the two-week culture, cells underwent a series of treatments. First, they were gently washed to remove any debris or residual medium. Next, the cells were fixed using a 4% paraformaldehyde solution for 15 minutes at 25°C. Following fixation, cells were stained with a 0.5% crystal violet solution (obtained from Sigma-Aldrich, USA) for 10 minutes at 25°C. Finally, the stained plates were examined under an optical microscope. Colonies, defined as clusters containing more than 50 cells, were identified and counted.

Flow cytometry

Cell apoptosis was stained utilizing the Annexin V-FITC kit (BioVision, USA). Subsequently, 1 × 105 cells were washed and then resuspended in 100 μL of binding buffer. Next, cells were added with 2 μL of Annexin V-FITC solution and cultivated for 15 minutes on ice in a light-free environment. Following this, 400 μL of PBS and 1 μL of PI were subjected to add into cells. Finally, apoptotic cells were analyzed by means of a flow cytometer.

Enzyme-linked immunosorbent assay (ELISA)

Tumor necrosis factor (TNF)-α, interleukin (IL)-1β and IL-10 were selected as key mediators of placental inflammation in GDM. The concentrations of TNF-α, IL-1β, as well as IL-10 in both mouse serum and cell supernatants were quantified based on the ELISA kits (R&D Systems, USA).

RNA pull-down assay

Cells were subjected to lysis and sonication. Then, the biotin-labeled MALAT1 probe was cultivated with C-1 magnetic beads (Thermo Fisher, USA) at 25°C for 2 hours to form probe-coated beads. Next, Cell lysate containing either the bio-MALAT1 probe or a biotinylated negative control (bio-NC) probe, was incubated overnight at 4°C. Following washing, the RNA bound to the beads was eluted and subsequently analyzed by means of RT-qPCR.

Dual luciferase reporter gene assay

The sequences of MALAT1 and miR-576-5p and HNRNPU 3'UTR and miR-576-5p were cloned and inserted into the pmirGLO plasmid to construct wild type (WT) MALAT1 and HNRNPU 3'UTR reporter gene plasmids (MALAT1-WT and HNRNPU 3'UTR-WT) and mutant type (MUT) MALAT1 and HNRNPU 3'UTR reporter gene plasmids (MALAT1-MUT and HNRNPU 3'UTR-MUT), respectively. The plasmids and miR-576-5p mimics were co-transfected into the cells for 24-hour incubation. The luciferase activity was measured using a luciferase activity detection kit.

RIP

Utilizing the Magna RIP kit (Millipore, USA), RIP experiments were performed. In short, cells were harvested and lysed in RIP buffer. Antibodies targeting Ago2 or IgG were then added to the lysates and cultivated with magnetic bead-antibody conjugates for 4 hours at 4°C. Subsequently, the bound RNA was purified, and the abundance of RNAs were quantified using RT-qPCR.

Statistical analysis

All experiments were replicated at least three times. Data analysis was performed based on GraphPad Prism 10.0. Continuous variables with normal distribution and homogeneity of variance are presented to be mean ± standard deviation (SD). Pairwise comparisons were conducted using the t-test, while one-way or two-way analysis of variance (ANOVA) was employed for comparisons among multiple groups, followed by Tukey's post hoc test for multiple comparisons. Statistical significance was defined as $P<0.05$ for all analyses.

Results

MALAT1 knockdown improves IR, pathological changes in pancreatic tissues and inflammation in GDM mice

A GDM mice model was built to assess MALAT1's impacts on IR, pathological changes in pancreatic tissues and inflammation in vivo.

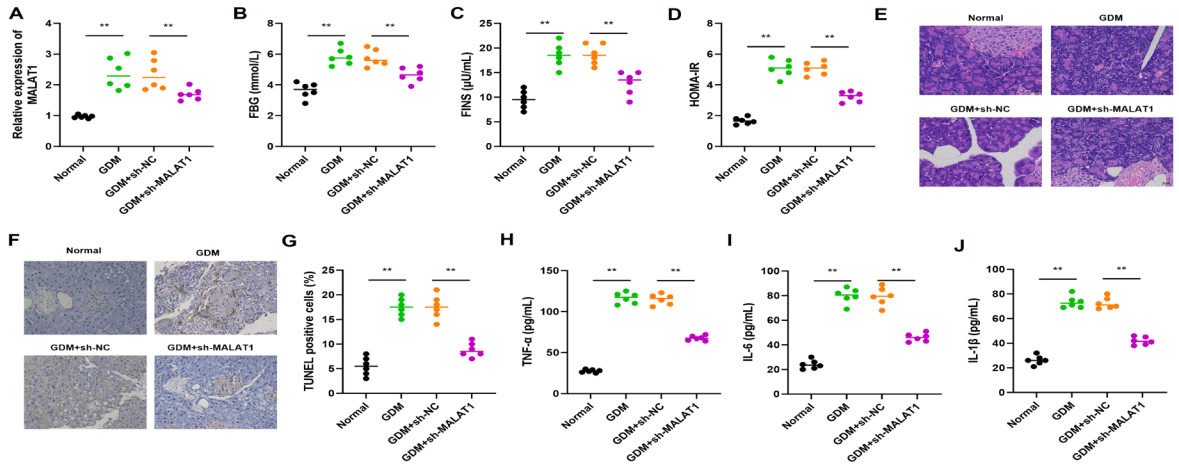

Figure 1 Knockdown of MALAT1 improves IR, pathological changes in pancreatic tissues and inflammation in GDM mice. Mice were divided into four groups, including normal, GDM, GDM+sh-NC and GDM+sh-MALAT1 groups, followed by (A) RT-qPCR detection of MALAT1 expression (n=6); (B) FBG level was detected using glucose oxidase-peroxidase method (n=6); (C) FINS level was detected using ELISA (n=6); (D) Quantitative analysis of HOMA-IR (n=6); (E) HE staining was performed to detect the pathological changes of pancreatic tissues (n=6); (F-G) TUNEL staining assessed cell apoptosis of pancreatic tissues (n=6); (H-J) ELISA detection of serum levels of TNF-α, IL-1α and IL-6 (n=6). **P<0.01.

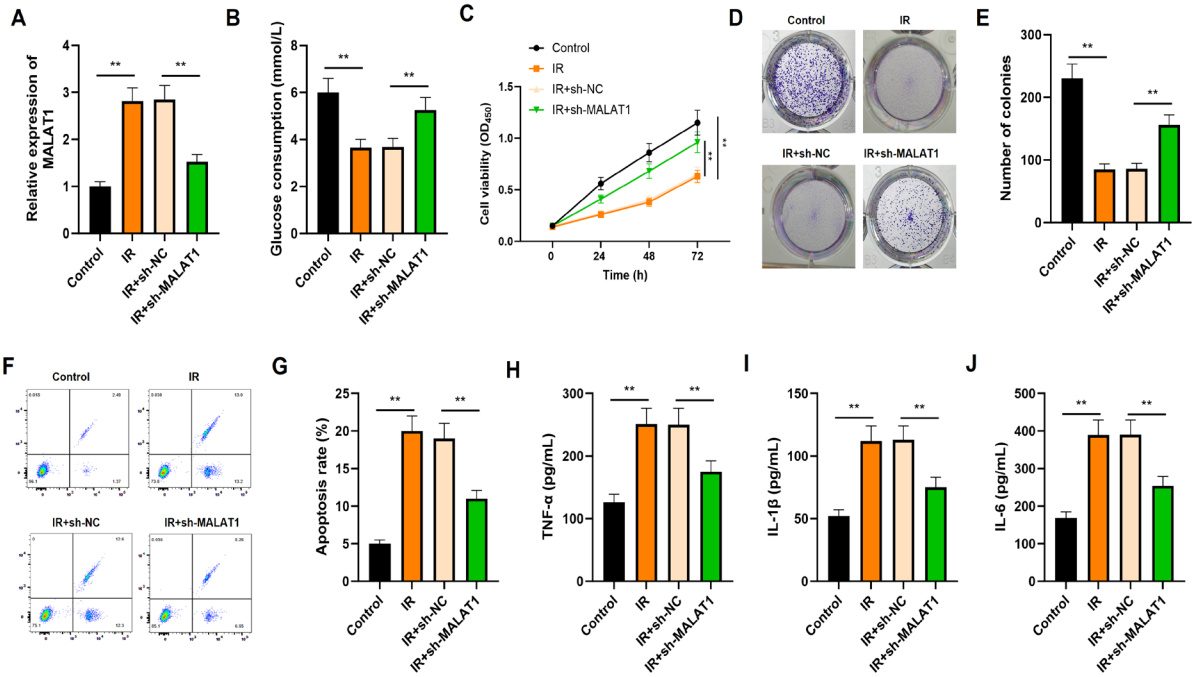

Figure 2 Silencing of MALAT1 attenuates IR, apoptosis and inflammation in trophoblast cells treated with insulin. HTR-8/SVneo cells were divided into four groups, including control, IR, IR+sh-NC and IR+sh-MALAT1 groups, followed by (A) RT-qPCR detection of MALAT1 expression (n=3); (B) Measurement of glucose consumption (n=3); (C) CCK-8 assay was used to detect cell viability (n=3); (D-E) Colony formation assay assessed the number of colonies (n=3); (F-G) Flow cytometry analysis measured cell apoptosis (n=3); (H-J) ELISA detection of levels of TNF-α, IL-1α and IL-6 (n=3). **P<0.01.

As displayed in Figure 1A, MALAT1 expression was apparently upregulated in GDM mice, however, after injection of sh-MALAT1, MALAT1 expression was significantly lessened in GDM mice. Besides, it was seen that in contrast to the normal group, FBG, FINS as well as HOMA-IR levels were elevated in the GDM mice, but their levels were diminished after MALAT1 silencing (Figure 1B-1D). Following HE staining of pancreatic tissue sections from mice, the islets in the normal group were observed as round or oval cell clusters with distinct boundaries, containing a high number of islets and abundant islet cells. In contrast, the GDM group exhibited pronounced islet atrophy, reduced islet cell counts, exacerbated inflammatory lesions, and increased vacuolar degeneration of β-cells. Notably, the GDM+sh-MALAT1 group demonstrated improved islet architecture, increased islet quantity and cellularity, attenuated inflammatory changes, and enhanced islet regeneration compared to the GDM group (Figure 1E). TUNEL staining results revealed a notable increase in cell apoptosis within pancreatic tissues in the GDM group when compared to the normal group. Conversely, the GDM+sh-MALAT1 group exhibited a definite reduction in pancreatic

 https://dx.doi.org/10.4314/mmj.v37i5.14

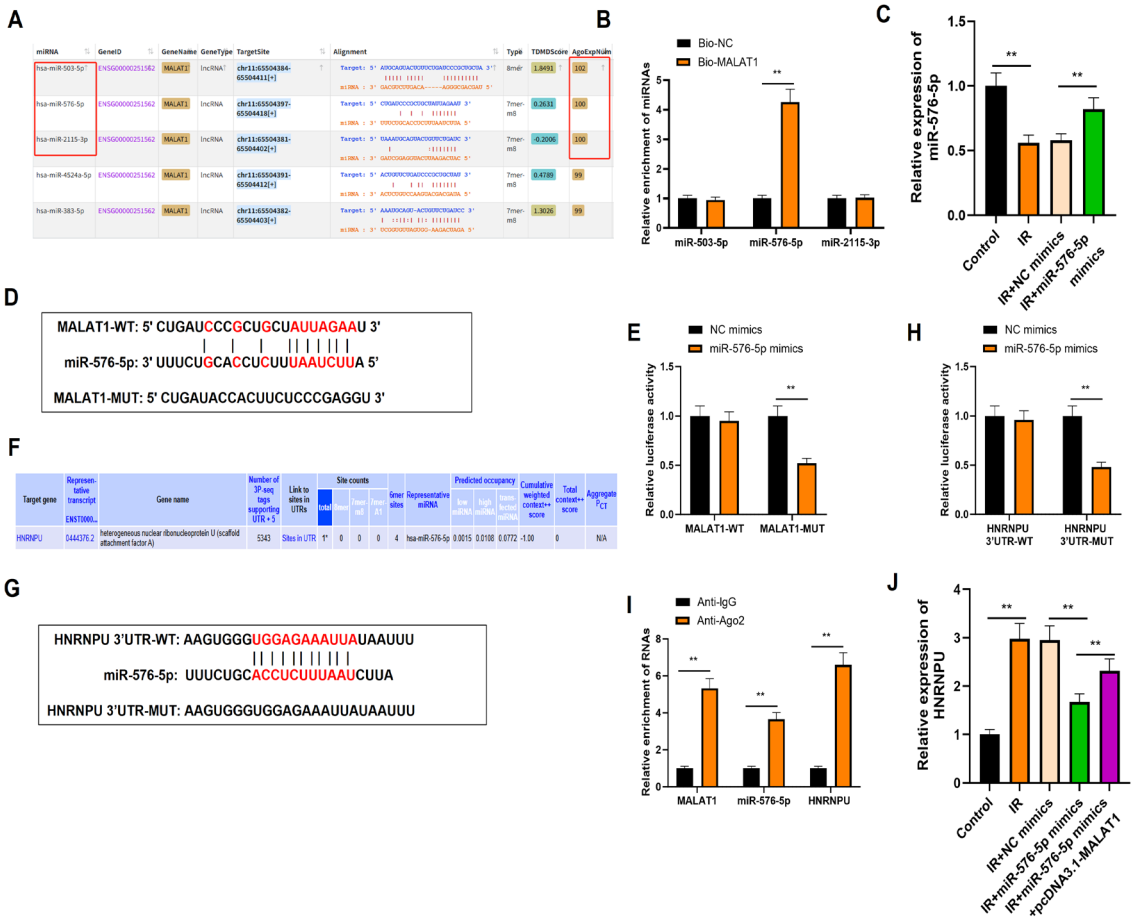

Figure 3 MALAT1 regulates HNRNPU expression via binding to miR-576-5p. (A) Prediction by the starBase website, three miRNAs of MALAT1 with AgoExpNum ≥100 were identified, namely miR-503-5p, miR-576-5p and miR-2115-3p. (B) RNA pull-down assay was performed to verify the binding between three miRNAs and MALAT1 (n=3). (C) RT-qPCR detection of miR-576-5p expression in HTR-8/SVneo cells including control, IR, IR+NC mimics and IR+miR-576-5p mimics groups (n=3). (D) Binding sites between miR-576-5p and MALAT1. (E) Dual luciferase reporter gene assay verified the impacts of miR-576-5p mimics on the luciferase activity of MALAT1-WT and MALAT1-MUT (n=3). (F) TargetScan website predicted that HNRNPU was the target mRNA of miR-576-5p with the highest total context++ score. (G) Binding sequences between HNRNPU 3'UTR and miR-576-5p. (H) Dual luciferase reporter gene assay verified the impacts of miR-576-5p mimics on the luciferase activity of HNRNPU 3'UTR-WT and HNRNPU 3'UTR-MUT (n=3). (I) RIP assay detected the enrichment of MALAT1, miR-576-5p and HNRNPU in Ago2 (n=3). (J) RT-qPCR detected HNRNPU expression in HTR-8/SVneo cells including control, IR, IR+NC mimics, IR+miR-576-5p mimics and IR+miR-576-5p mimics+pcDNA3.1-MALAT1 groups (n=3). **P<0.01.

cell apoptosis relative to the GDM group (Figure 1F-1G). Consistent with the pancreatic islet atrophy and inflammatory lesions observed in HE staining (Figure 1E), serum levels of pro-inflammatory cytokines (TNF-α, IL-1β, and IL-6) were significantly elevated in GDM mice, suggesting systemic and local immune activation (Figure 1H-J). Notably, TNF-α and IL-1β are known to promote macrophage infiltration and β-cell dysfunction in diabetic pancreata. The reduction of these cytokines upon MALAT1 knockdown implies a potential suppression of immune cell recruitment, possibly contributing to the improved islet morphology and insulin sensitivity. Although direct evidence of immune infiltration (e.g., F4/80+ macrophages) was not assessed here, the coordinated changes in cytokine levels and tissue pathology align with established models of GDM-associated pancreatic inflammation.

Silencing of MALAT1 attenuates IR, apoptosis and inflammation in trophoblast cells treated with insulin

The role of MALAT1 in IR of GDM was investigated by stimulating IR in HTR-8/SVneo cells with insulin. After insulin treatment, MALAT1 expression was elevated. Next, we downregulated MALAT1 expression in HTR8/SVneo cells via transfecting with sh-MALAT1, and found that the upregulated MALAT1 expression caused by insulin treatment was downregulated (Figure 2A). The MALAT1's impact on IR was assessed by detecting glucose consumption. As displayed in Figure 2B, insulin treatment promoted apparent IR in HTR8/SVneo cells, but was weakened following MALAT1 depletion. Besides, we observed that insulin treatment significantly reduced cell proliferation, but after transfection of sh-MALAT1, the reduced cell proliferation in insulin-treated HTR8/SVneo cells were increased (Figure 2C-2E). Meanwhile, the apoptosis rate was augmented in insulin-treated HTR8/SVneo cells, but this effect was abolished after MALAT1 silencing (Figure 2F-2G). In addition, insulin treatment elevated TNF-α, IL-1β as well as IL-6 levels, but MALAT1 depletion lessened their levels (Figure 2H-2J).

MALAT1 regulates HNRNPU expression through binding to miR-576-5p

Prediction by the starBase website (https://rnasysu.com/encori/), we identified three miRNAs of MALAT1 with AgoExpNum ≥100, namely miR-503-5p, miR-576-5p and miR-2115-3p (Figure 3A). Through RNA pull-down assay, we discovered only miR-576-5p was significantly abundant in bio-MALAT1 probe, while other miRNAs were unchanged between the bio-MALAT1 and bio-NC groups (Figure 3B).

https://dx.doi.org/10.4314/mmj.v37i5.14

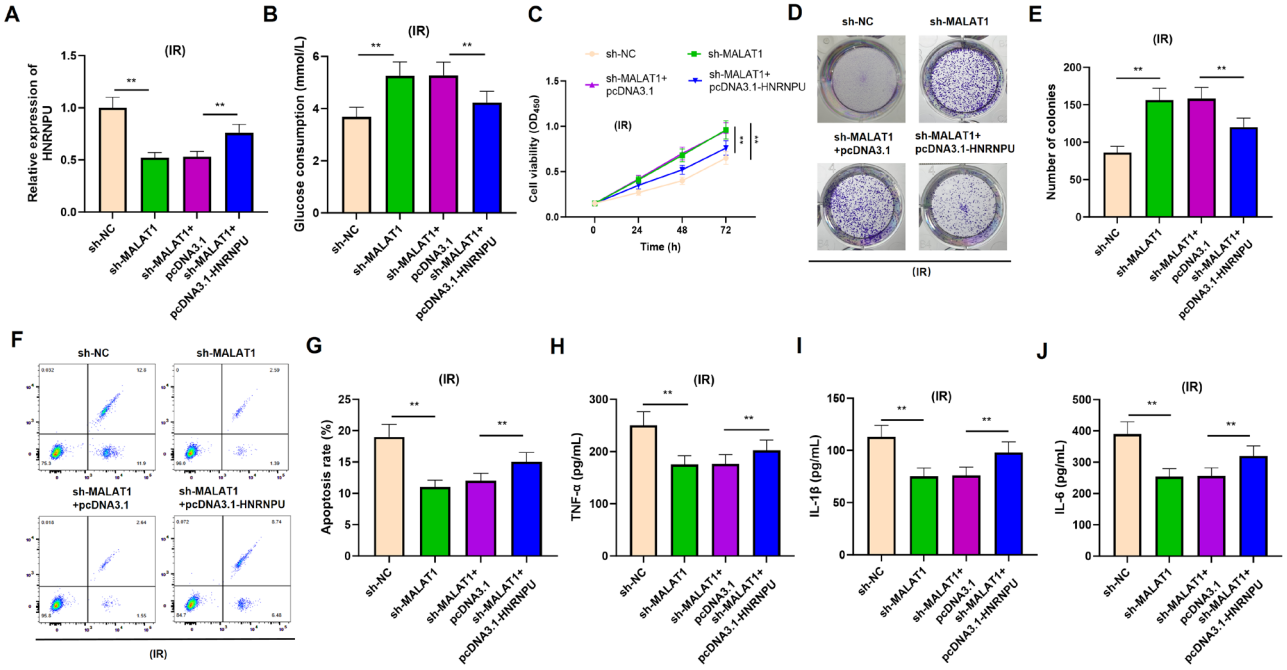

Figure 4 MALAT1 affects IR, apoptosis and inflammation in trophoblast cells treated with insulin via regulating HNRNPU. Insulin-treated HTR8/SVneo cells were divided into four groups, including sh-NC, sh-MALAT1, sh-MALAT1+pcDNA3.1 and sh-MALAT1+pcDNA3.1-HNRNPU, followed by (A) RT-qPCR detected HNRNPU expression (n=3); (B) Measurement of glucose consumption (n=3); (C) CCK-8 assay was used to detect cell viability (n=3); (D-E) Colony formation assay assessed the number of colonies (n=3); (F-G) Flow cytometry analysis measured cell apoptosis (n=3); (H-J) ELISA detection of levels of TNF-α, IL-1α and IL-6 (n=3). **P<0.01.

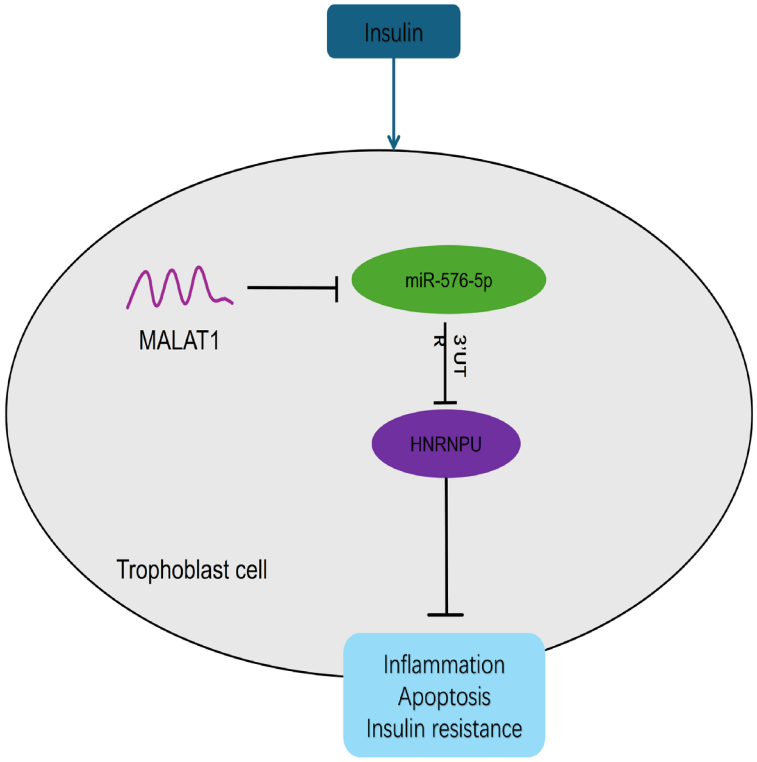

Figure 5 Overall mechanisms of action based on the results of present study

RT-qPCR analysis displayed that miR-576-5p expression was downregulated in insulin-treated HTR8/SVneo cells. Then, we elevated miR-576-5p expression in HTR8/SVneo cells via transfecting with miR-576-5p mimics, and discovered that the reduced miR-576-5p expression in insulin-treated HTR8/SVneo cells was enhanced (Figure 3C). The binding sites between MALAT1 and miR-576-5p were revealed in Figure 3D, and subsequent dual luciferase reporter gene assay validated that miR-576-5p overexpression obviously diminished the luciferase activity of MALAT1-WT, whereas did not affect that of MALAT1-MUT (Figure 3E). Utilizing TargetScan website (https://www.targetscan.org/vert_80/), we predicted that HNRNPU was the target mRNA of miR-576-5p with the highest total context++ score (Figure 3F), and the binding sequences between HNRNPU 3'UTR and miR-576-5p were indicated in Figure 3G. Based on dual

luciferase reporter gene assay results, we observed that miR-576-5p mimics led to a reduction in the luciferase activity of HNRNPU 3'UTR-WT, but did not change the luciferase activity of HNRNPU 3'UTR-MUT (Figrue 3H). RIP assay using an Ago2 antibody further confirmed that MALAT1, miR-576-5p and HNRNPU were specifically abundant in Ago2 antibody-linked complex (Figure 3I). In addition, we observed that HNRNPU was high-expressed in insulin-treated HTR8/SVneo cells but downregulated following transfection of miR-576-5p mimics. More importantly, the reduced HNRNPU expression caused by miR-576-5p mimics was reversed following co-transfection of pcDNA3.1-MALAT1 (Figure 3J).

MALAT1 affects IR, apoptosis and inflammation in trophoblast cells treated with insulin via upregulating HNRNPU

Furthermore, we overexpressed HNRNPU in HTR8/SVneo cells, and found that the reduced HNRNPU expression regulated by MALAT1 silencing in insulin-treated HTR8/SVneo cells was enhanced after co-transfection of pcDNA3.1-HNRNPU (Figure 4A). Then, we performed rescue assays to verify that MALAT1 affected IR, apoptosis along with inflammation in trophoblast cells treated with insulin through modulating HNRNPU. It was seen in Figure 4B that the elevated glucose consumption induced by MALAT1 silencing was offset after co-transfection of pcDNA3.1-HNRNPU (Figure 4B). Besides, HNRNPU overexpression rescued the increased proliferation ability regulated by MALAT1 depletion in insulin-treated HTR8/SVneo cells (Figure 4C-4E). Meanwhile, in insulin-treated HTR8/SVneo cells, the diminished apoptosis rate medicated by MALAT1 downregulation was restored after simultaneous HNRNPU elevation (Figure 4F-4G). Moreover, the reduced levels of TNF-α, IL-1β as well as IL-6 regulated by MALAT1 deficiency were counteracted upon co-transfection of pcDNA3.1-HNRNPU (Figure 4H-4J).

Discussion

GDM stands as the most prevalent complication encountered during pregnancy, exerting profound adverse impacts on both the mother and the developing fetus. This condition is associated with a spectrum of short- and long-term complications, including macrosomia, fetal respiratory distress, and even stillbirth[22]. Currently, there is a broad consensus that the heightened IR observed in the body is the central issue underpinning GDM, serving as its widely acknowledged pathophysiological foundation[23]. A previous study has reported that downregulated MALAT1 impedes the proliferation, invasion as well as migration of placental trophoblastic cells in GDM[24], but the precise role and mechanisms of MALAT1 in modulating IR present elusive. In the present research, we elucidated that MALAT1 exacerbated IR, inflammation, as well as apoptosis in GDM by orchestrating the miR-576-5p/HNRNPU axis.

First of all, this study established both GDM mouse model and IR cell model to explore MALAT1's role in regulating IR, inflammation as well as apoptosis in GDM. We demonstrated that knocking down MALAT1 expression significantly diminished FBG, FINS along with HOMA-IR levels in GDM mice, thereby facilitating the insulin sensitivity of GDM mice. Meanwhile, MALAT1 knockdown revised the reduced glucose consumption mediated by insulin treatment in HTR8/SVneo cells. Consistently, Yan et al. suggested that MALAT1 promoted hepatic steatosis and IR in a T2DM mouse model[25]. Liu et al. studied the potential mechanism of exercise-mediated IR in T2DM, and indicated that exercise protected against IR via regulating MALAT1 expression[26]. Therefore, the regulatory effect of MALAT1 deficiency on glucose metabolism in placental trophoblast cells (HTR8/SVneo) further indicates that MALAT1 has a conserved pro-resistance function in metabolically sensitive tissues.

The secretion of inflammatory cytokines has a pivotal role in IR development and is intricately linked to the pathogenesis and associated complications of GDM[27]. Among these cytokines, the immune-inflammatory mediator TNF-α has been implicated in the onset of IR. Furthermore, serological abnormalities in cytokines like IL-1β and IL-6 have been extensively documented in patients with GDM[28]. In our study, we discovered that the apoptosis rate and serum levels of TNF-α, IL-1β as well as IL-6 were enhanced in the GDM mice, but this phenomenon was reversed after MALAT1 depletion. Simultaneously, insulin treatment elevated the apoptosis rate and TNF-α, IL-1β as well as IL-6 levels in HTR8/SVneo cells, but MALAT1 depletion diminished the apoptosis rate and TNF-α, IL-1β and IL-6 levels. Likewise, Wang et al. pointed out that MALAT1 depletion attenuated high-glucose-stimulated inflammatory reaction in human retinal vascular endothelial cells[29]. Zhao et al. suggested that knockdown of MALAT1 suppressed inflammatory response and the pyroptosis of mouse microglia[30]. Du et a. suggested that silencing of MALAT1 inhibited the hippocampal inflammatory response in T2DM with obstructive sleep apnea[31]. In contrast, the regulation of apoptosis in HTR8/SVneo cells by MALAT1 in this study did not involve activation of the inflammasome, suggesting that the inflammatory response in GDM may be more dependent on the classical TNF-α/NF-κB pathway.

Recent literatures have uncovered that dysregulated lncRNA□ mRNA network based on ceRNAs is implicated in GDM[32]. MALAT1 has been found to accelerates diabetic nephropathy progression through interacting with miR-15b-5p to modulate TLR4 expression[33]. Besides, it has been proved that MALAT1 depletion mitigates high-glucose-stimulated angiogenesis via binding to miR-205-5p to modulate VEGF-A expression in diabetic retinopathy[34]. Similarly, our study also used bioinformatic analysis to predict the miRNAs of MALAT1. It was discovered that miR-576-5p bound to MALAT1, and miR-576-5p expression was low-expressed in insulin-treated HTR8/SVneo cells. Furthermore, we also proved that HNRNPU was the target mRNA of miR-576-5p, and the findings of rescue experiment further validated that MALAT1 worked to be a ceRNA for miR-576-5p to affect HNRNPU expression.

Heterogeneous nuclear ribonucleoprotein U (HNRNPU) is a distinct category of RNA-binding protein, characterized by its high-affinity interactions with RNA, DNA, and a diverse array of proteins. This versatile protein plays multifarious roles in cellular processes, encompassing RNA splicing, preservation of RNA stability, modulation of gene transcription, and chromatin organization[35]. HNRNPU is ubiquitously expressed throughout the human body and has participated in a spectrum of biological phenomena, containing cell apoptosis as well as inflammatory responses[36,37]. Many studies have indicated the involvement of HNRNPU in diabetes-related diseases, such as diabetic nephropathy[38] and diabetic foot ulcer[39].

However, its expression and role in GDM remains unclear. In our study, we performed rescue assays to further validate that MALAT1 promotes IR, apoptosis as well as inflammation in trophoblast cells following insulin treatment via modulating HNRNPU, suggesting targeting the MALAT1/miR-576-5p/HNRNPU axis may be a promising treatment modality of GDM. GDM is increasingly recognized as a state of chronic low-grade inflammation, where aberrant immune responses contribute to insulin resistance and β-cell dysfunction. Our study identifies MALAT1 as a key regulator of inflammatory cascades in GDM, bridging lncRNA-mediated immune dysregulation with metabolic impairment. The elevated levels of TNF-α, IL-1β, and IL-6 in GDM mice align with prior reports of cytokine-driven IR in gestational diabetes. Notably, MALAT1 knockdown attenuated these inflammatory markers, suggesting its role in potentiating innate immune activation.

While our data highlight the MALAT1/miR-576-5p/HNRNPU axis, future studies should explore direct interactions between HNRNPU and immune signaling pathways (e.g., NF-ϰB or NLRP3 inflammasome) in GDM. A limitation of this work is the lack of mechanistic validation in immune cells (e.g., macrophages or T cells), which are critical contributors to placental inflammation in GDM. Nevertheless, our findings implicate MALAT1 as a potential biomarker for immune-metabolic crosstalk in GDM. In addition, our findings are derived from a mouse model of GDM and in vitro trophoblast cell cultures. While these systems mimic key pathological features of GDM, they may not fully recapitulate the complexity of human pregnancy, including placental-fetal interactions and maternal-fetal immune crosstalk. Future studies using human placental tissues or primary trophoblasts from GDM pregnancies are needed to validate translational relevance.

In conclusion, our study demonstrates that MALAT1 promotes IR, apoptosis and inflammation in GDM through its regulatory influence on the miR-576-5p/HNRNPU axis (Figure 5). This paper contributes significantly to our comprehension of potential therapeutic strategies for GDM, offering fresh perspectives and innovative insights that could pave the way for novel treatment approaches for this condition.

Declarations

Ethics approval and consent to participate

This study did not involve human participants or identifiable personal data. All animal experiments were conducted in accordance with institutional guidelines and were approved by the Ethics Committee of Xuyi County People's Hospital, and the approval number was XY20230019[L]. Informed consent is not applicable.

Consent for publication

Not applicable.

Availability of data and materials

All data supporting the findings of this study are included within the article. Additional datasets are available from the corresponding author upon reasonable request.

Competing interests

The authors declare that they have no competing interests.

Funding

This research received no specific grant from any funding agency in the public, commercial, or not-for-profit sectors.

Authors' contributions

Hui Ding designed the study, performed experiments, and drafted the manuscript. Anna Zhao contributed to data analysis and figure preparation. Xia Chen performed experiments and data verification. Yanli Niu managed experimental materials and data collection. Yuanyuan Wang conducted statistical analysis and contributed to manuscript revision. Xiao Chen assisted with supplementary experiments and reference formatting. Hong Yang conceived and supervised the study, interpreted the results, and critically revised the manuscript. All authors read and approved the final version of the manuscript.

Acknowledgements

None.

References

1.Ye W, Luo C, Huang J, Li C, Liu Z, Liu F. Gestational diabetes mellitus and adverse pregnancy outcomes: systematic review and meta-analysis. Bmj. 2022;377:e067946.

2.Sweeting A, Wong J, Murphy HR, Ross GP. A Clinical Update on Gestational Diabetes Mellitus. Endocr Rev. 2022;43(5):763-93.

3.Rasmussen L, Poulsen CW, Kampmann U, Smedegaard SB, Ovesen PG, Fuglsang J. Diet and Healthy Lifestyle in the Management of Gestational Diabetes Mellitus. Nutrients. 2020;12(10).

4.Choudhury AA, Devi Rajeswari V. Gestational diabetes mellitus - A metabolic and reproductive disorder. Biomed Pharmacother. 2021;143:112183.

5.Oskovi-Kaplan ZA, Ozgu-Erdinc AS. Management of Gestational Diabetes Mellitus. Adv Exp Med Biol. 2021;1307:257-72.

6.Lee SH, Park SY, Choi CS. Insulin Resistance: From Mechanisms to Therapeutic Strategies. Diabetes Metab J. 2022;46(1):15-37.

7.Martín-Estal I, Castorena-Torres F. Gestational Diabetes Mellitus and Energy-Dense Diet: What Is the Role of the Insulin/IGF Axis? Front Endocrinol (Lausanne). 2022;13:916042.

8.Chen LL, Kim VN. Small and long non-coding RNAs: Past, present, and future. Cell. 2024;187(23):6451-85.

9.Nemeth K, Bayraktar R, Ferracin M, Calin GA. Non-coding RNAs in disease: from mechanisms to therapeutics. Nat Rev Genet. 2024;25(3):211-32.

10.Yang J, Ariel F, Wang D. Plant long non-coding RNAs: biologically relevant and mechanistically intriguing. J Exp Bot. 2023;74(7):2364-73.

11.Ratti M, Lampis A, Ghidini M, Salati M, Mirchev MB, Valeri N, et al. MicroRNAs (miRNAs) and Long Non-Coding RNAs (lncRNAs) as New Tools for Cancer Therapy: First Steps from Bench to Bedside. Target Oncol. 2020;15(3):261-78.

12.Chen B, Dragomir MP, Yang C, Li Q, Horst D, Calin GA. Targeting non-coding RNAs to overcome cancer therapy resistance. Signal Transduct Target Ther. 2022;7(1):121.

13.Li C, Ni YQ, Xu H, Xiang QY, Zhao Y, Zhan JK, et al. Roles and mechanisms of exosomal non-coding RNAs in human health and diseases. Signal Transduct Target Ther. 2021;6(1):383.

14.Coan M, Haefliger S, Ounzain S, Johnson R. Targeting and engineering long non-coding RNAs for cancer therapy. Nat Rev Genet. 2024;25(8):578-95.

15.Zhao Y, Ning J, Teng H, Deng Y, Sheldon M, Shi L, et al. Long noncoding RNA Malat1 protects against osteoporosis and bone metastasis. Nat Commun. 2024;15(1):2384.

16.Taylor AD, Hathaway QA, Meadows EM, Durr AJ, Kunovac A, Pinti MV, et al. Diabetes mellitus disrupts lncRNA Malat1 regulation of cardiac mitochondrial genome-encoded protein expression. Am J Physiol Heart Circ Physiol. 2024;327(6):H1503-h18.

17.Goyal B, Yadav SRM, Awasthee N, Gupta S, Kunnumakkara AB, Gupta SC. Diagnostic, prognostic, and therapeutic significance of long non-coding RNA MALAT1 in cancer. Biochim Biophys Acta Rev Cancer. 2021;1875(2):188502.

18.Zhang Y, Wu H, Wang F, Ye M, Zhu H, Bu S. Long non-coding RNA MALAT1 expression in patients with gestational diabetes mellitus. Int J Gynaecol Obstet. 2018;140(2):164-9.

19.Abdulle LE, Hao JL, Pant OP, Liu XF, Zhou DD, Gao Y, et al. MALAT1 as a Diagnostic and Therapeutic Target in Diabetes-Related Complications: A Promising Long-Noncoding RNA. Int J Med Sci. 2019;16(4):548-55.

20.Chen SH, Liu XN, Peng Y. MicroRNA-351 eases insulin resistance and liver gluconeogenesis via the PI3K/AKT pathway by inhibiting FLOT2 in mice of gestational diabetes mellitus. J Cell Mol Med. 2019;23(9):5895-906.

21.Bai Y, Du Q, Zhang L, Li L, Wang N, Wu B, et al. Silencing of ANGPTL8 Alleviates Insulin Resistance in Trophoblast Cells. Front Endocrinol (Lausanne). 2021;12:635321.

22.Wicklow B, Retnakaran R. Gestational Diabetes Mellitus and Its Implications across the Life Span. Diabetes Metab J. 2023;47(3):333-44.

23.Hashemipour S, Zohal M, Modarresnia L, Kolaji S, Panahi H, Badri M, et al. The yield of early-pregnancy homeostasis of model assessment -insulin resistance (HOMA-IR) for predicting gestational diabetes mellitus in different body mass index and age groups. BMC Pregnancy Childbirth. 2023;23(1):822.

24.Zhang Y, Qu L, Ni H, Wang Y, Li L, Yang X, et al. Expression and function of lncRNA MALAT1 in gestational diabetes mellitus. Adv Clin Exp Med. 2020;29(8):903-10.

25.Yan C, Chen J, Chen N. Long noncoding RNA MALAT1 promotes hepatic steatosis and insulin resistance by increasing nuclear SREBP-1c protein stability. Sci Rep. 2016;6:22640.

26.Liu SX, Zheng F, Xie KL, Xie MR, Jiang LJ, Cai Y. Exercise Reduces Insulin Resistance in Type 2 Diabetes Mellitus via Mediating the lncRNA MALAT1/MicroRNA-382-3p/Resistin Axis. Mol Ther Nucleic Acids. 2019;18:34-44.

27.Wang Y, Song M, Qi BR. Effects of insulin aspart and metformin on gestational diabetes mellitus and inflammatory markers. World J Diabetes. 2023;14(10):1532-40.

28.Gayatri V, Krishna Prasad M, Mohandas S, Nagarajan S, Kumaran K, Ramkumar KM. Crosstalk between inflammasomes, inflammation, and Nrf2: Implications for gestational diabetes mellitus pathogenesis and therapeutics. Eur J Pharmacol. 2024;963:176241.

29.Wang Y, Wang L, Guo H, Peng Y, Nie D, Mo J, et al. Knockdown of MALAT1 attenuates high-glucose-induced angiogenesis and inflammation via endoplasmic reticulum stress in human retinal vascular endothelial cells. Biomed Pharmacother. 2020;124:109699.

30.Zhao N, Hua W, Liu Q, Wang Y, Liu Z, Jin S, et al. MALAT1 knockdown alleviates the pyroptosis of microglias in diabetic cerebral ischemia via regulating STAT1 mediated NLRP3 transcription. Mol Med. 2023;29(1):44.

31.Du P, Wang J, Han Y, Feng J. Blocking the LncRNA MALAT1/miR-224-5p/NLRP3 Axis Inhibits the Hippocampal Inflammatory Response in T2DM With OSA. Front Cell Neurosci. 2020;14:97.

32.Li Y, Liu Y, Yao X, Wang H, Shi Z, He M. METTL14-mediated lncRNA XIST silencing alleviates GDM progression by facilitating trophoblast cell proliferation and migration via the miR-497-5p/FOXO1 axis. J Biochem Mol Toxicol. 2024;38(1):e23621.

33.Yang Z, Song D, Wang Y, Tang L. lncRNA MALAT1 Promotes Diabetic Nephropathy Progression via miR-15b-5p/TLR4 Signaling Axis. J Immunol Res. 2022;2022:8098001.

34.Tan A, Li T, Ruan L, Yang J, Luo Y, Li L, et al. Knockdown of Malat1 alleviates high-glucose-induced angiogenesis through regulating miR-205-5p/VEGF-A axis. Exp Eye Res. 2021;207:108585.

35.Shi ZD, Hao L, Han XX, Wu ZX, Pang K, Dong Y, et al. Targeting HNRNPU to overcome cisplatin resistance in bladder cancer. Mol Cancer. 2022;21(1):37.

36.Lu Y, Liu X, Xie M, Liu M, Ye M, Li M, et al. The NF-κB-Responsive Long Noncoding RNA FIRRE Regulates Posttranscriptional Regulation of Inflammatory Gene Expression through Interacting with hnRNPU. J Immunol. 2017;199(10):3571-82.

37.Wang X, Xu J, Li Q, Zhang Y, Lin Z, Zhai X, et al. RNA-binding protein hnRNPU regulates multiple myeloma resistance to selinexor. Cancer Lett. 2024;580:216486.

38.Zhang C, Zhao H, Yan Y, Li Y, Lei M, Liu Y, et al. LncRNA evf-2 Exacerbates Podocyte Injury in Diabetic Nephropathy by Inducing Cell Cycle Re-entry and Inflammation Through Distinct Mechanisms Triggered by hnRNPU. Adv Sci (Weinh). 2024;11(47):e2406532.

39.Wang Z, Xu H, Xue B, Liu L, Tang Y, Wang Z, et al. MSC-derived exosomal circMYO9B accelerates diabetic wound healing by promoting angiogenesis through the hnRNPU/CBL/KDM1A/VEGFA axis. Commun Biol. 2024;7(1):1700.